AGU PUBLICATIONS

Tectonics

RESEARCH ARTICLE
10.1002/2016TC004345

Key Points:
- Rocks above a detachment fault in western Arizona contain folds that reflect shortening in the same direction as regional extension
- Folded syn-extension strata are truncated by the detachment fault, indicating that folding occurred during the period of extension
- Application of critical-taper theory indicates that shortening would occur with appropriate surface slope and very low fault friction

Correspondence to:
J. E. Spencer,
spencer7@email.arizona.edu

Citation:
Spencer, J. E., S. J. Reynolds, R. J. Scott, and S. M. Richard (2016), Shortening in the upper plate of the Buckskin-Rawhide extensional detachment fault, southwestern U.S., and implications for stress conditions during extension, *Tectonics*, *35*, 3119–3136, doi:10.1002/2016TC004345.

Received 19 AUG 2016
Accepted 6 DEC 2016
Accepted article online 10 DEC 2016
Published online 29 DEC 2016

Shortening in the upper plate of the Buckskin-Rawhide extensional detachment fault, southwestern U.S., and implications for stress conditions during extension

Jon E. Spencer[1], Stephen J. Reynolds[2], Robert J. Scott[3], and Stephen M. Richard[1]

[1]Department of Geosciences, University of Arizona, Tucson, Arizona, USA, [2]Department of Geology, Arizona State University, Phoenix, Arizona, USA, [3]ARC Centre of Excellence in Ore Deposits, University of Tasmania, Hobart, Tasmania, Australia

Abstract Detailed geologic mapping in the Buckskin, Rawhide, and Artillery Mountains in western Arizona identified numerous folds in Oligocene-Miocene strata above the Buckskin-Rawhide extensional detachment fault. The folds are above or adjacent to the Harcuvar metamorphic core complex, which was uplifted and exposed by top-northeast normal faulting and penetrative shearing at ~27–9 Ma. Strata deposited during extension were folded, and the folds are truncated by the detachment fault, demonstrating that folding occurred during the period of extensional faulting. Fold axes are approximately perpendicular to regional extension direction. In two of the four areas of folding described here, alluvial-fan deposits derived partially from lower plate mylonitic rocks are the stratigraphically highest folded strata. Folding could have occurred above low-angle normal faults with curved or ramp-flat geometries, but fold abundance, large size, high degree of closure, and steep northeastward dips of the northeast limbs of anticlines lead us to consider the possibility that at least some folds reflect local shortening in the same direction as regional extension. Application of critical-taper theory to an extensional wedge with very low basal friction indicates that wedge shortening would be expected if the wedge developed a sufficient surface slope that was downhill away from the wedge tip. Such a slope could have developed late during extension either because core-complex uplift tilted the wedge away from the core complex or because alluvial fans shed off the core complex produced such a slope. In either case, wedge shortening would promote core-complex denudation.

1. Introduction

Continental metamorphic core complexes consist of mylonitic crystalline rocks that are overlain and flanked by gently to moderately dipping normal faults known as detachment faults. Mylonitic rocks were uplifted and exhumed from middle-crustal depths during tectonic extension and displacement on the detachment faults and related shear zones [e.g., *Davis et al.*, 1986]. The effectiveness of tectonic exhumation in some complexes, with essentially complete denudation, is not well understood but is likely related to a very low coefficient of friction on extensional detachment faults. The Buckskin and Rawhide Mountains are part of the giant Harcuvar metamorphic core complex in western Arizona, USA, and are flanked to the northeast by upper plate rocks in the Artillery Mountains. Detailed mapping of upper plate strata in these ranges identified numerous folds with axes perpendicular to extension direction. The folds affect the entire syn-extension stratigraphic sections in these areas but are truncated by the underlying detachment fault, demonstrating that folding occurred late during the period of detachment faulting.

In this paper we first document the folds and their geologic setting within the core complex, and then evaluate possible causes of folding. Some folds likely resulted from displacement above bends in underlying normal faults, analogous to such folds in thrust belts, or to reverse drag above listric normal faults [e.g., *Scott and Lister*, 1992; *Schlische*, 1995; *Janecke et al.*, 1998; *Brandes and Tanner*, 2014]. Our structural evaluation suggests, however, that at least some of the folds record simple shortening. Application of critical-taper theory [*Dahlen*, 1984; *Xiao et al.*, 1991] to an extensional wedge with low internal and basal coefficients of friction predicts wedge shortening if surface slope in upper plate rocks is just a few degrees (downhill) away from the core complex. This leads to the conclusion that wedge shortening was potentially triggered by development of such a slope, which could have resulted from rapid uplift and arching of the footwall or from development of alluvial fans derived from the emerging core complex. In either case, potential energy due to the surface slope would be available for wedge shortening, just as it would be available for wedge extension if surface slope in the wedge is downhill toward the wedge tip.

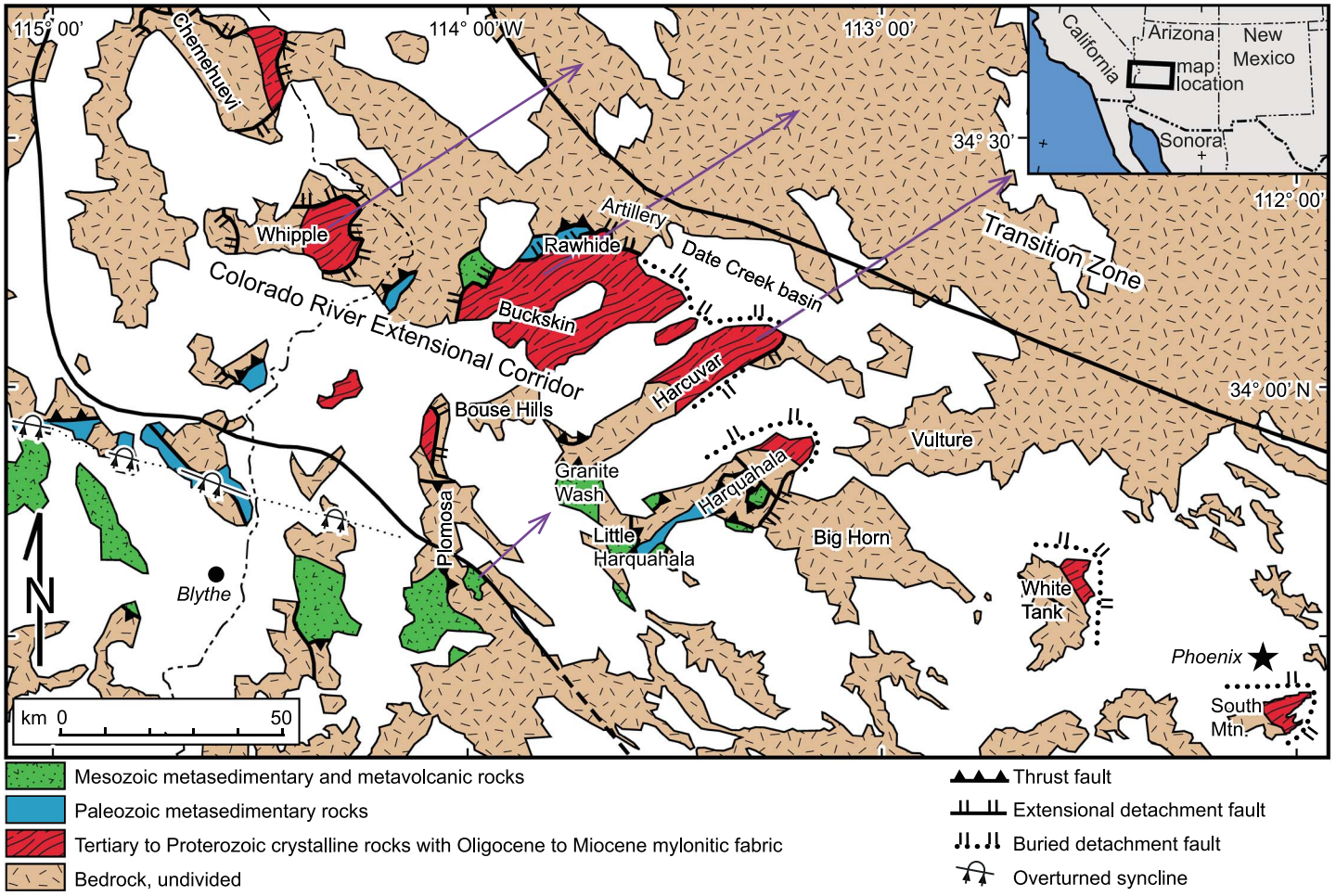

Figure 1. Simplified geologic map of the southern and central part of the Colorado River extensional corridor, which is bounded by the heavy black lines. The mylonitic part of the Rawhide, Buckskin, Harcuvar, and Harquahala Mountains make up the Harcuvar metamorphic core complex. Restoration of extension indicated by arrows would place mylonitic core-complex rocks beneath the central Arizona Transition Zone, an area bordering the Colorado Plateau that is only slightly extended at the surface [*Spencer and Reynolds*, 1991].

2. Geologic Setting

The Buckskin, Rawhide, and Artillery Mountains are located in the central part of the Colorado River extensional corridor in the Mojave-Sonora desert region of the southwestern U.S. (Figure 1) [*Howard and John*, 1987; *Spencer and Reynolds*, 1989a]. Severe extension in the corridor at ~27–9 Ma uncovered some of Earth's largest metamorphic core complexes. Total extension, estimated at ~90 km within the central part of the corridor, affected an area with an initial width of as little as perhaps 10 km [*Spencer and Reynolds*, 1991]. Mylonitic core-complex rocks were exhumed by tens of kilometers of top-northeast displacement on an extensional detachment-fault system and distributed shearing within its mylonitic and brecciated footwall rocks [e.g., *Rehrig and Reynolds*, 1980; *Reynolds and Spencer*, 1985; *John*, 1987; *Davis and Lister*, 1988; *Singleton and Mosher*, 2012]. The exceptionally large exposures resulted from minimal extension within the hanging wall crystalline rocks and insufficient sedimentation to bury the emerging footwall. Exposure of mylonitic footwall rocks occurred late during extension as indicated by the large fraction of mylonitic clasts in the stratigraphically highest, faulted conglomerate unit. Geomorphology has not been greatly modified following tectonic extension because of arid desert conditions, low elevations, partial burial by basalt flows, and only minor younger faulting and magmatism [*Spencer and Reynolds*, 1991].

The Harcuvar metamorphic core complex includes mylonitic crystalline rocks in the Rawhide, Buckskin, Little Buckskin, Harcuvar, and Harquahala Mountains (Figure 2). Mylonitic rocks are bounded upward and laterally by the corrugated Buckskin-Rawhide-Bullard-Eagle Eye extensional detachment fault. A variety of structural

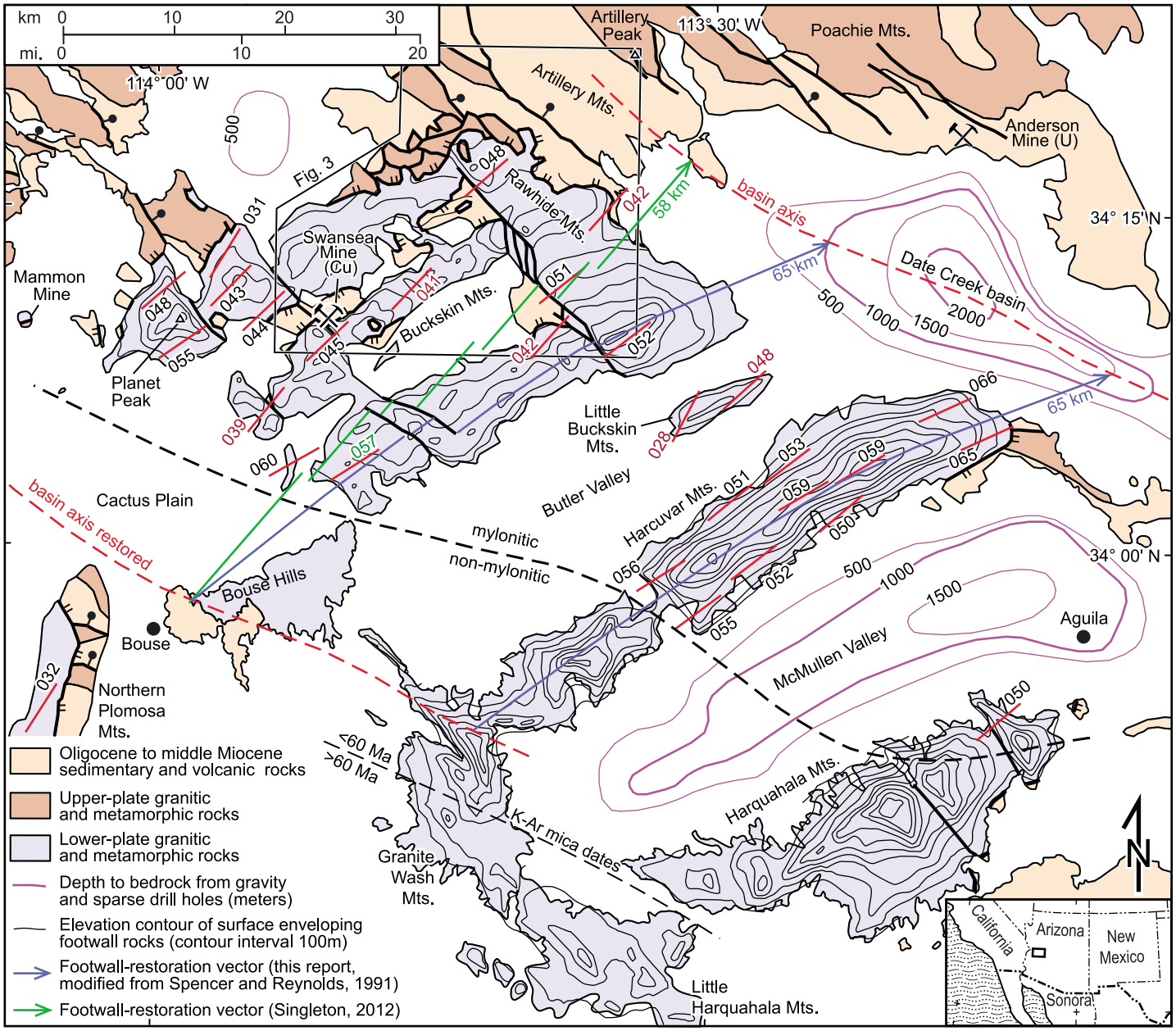

Figure 2. Simplified geologic map of the Harcuvar core complex. The red line segments represent average orientation of mylonitic lineations in each area. Numbers adjacent to each segment indicate average trend, which in some cases is transposed 180° to the northeast quadrant for comparison (opposite to plunge). Numbers in black are derived from data collected by the authors. Number in green is from *Marshak and Vander Meulen* [1989]. Numbers in red are from *Singleton* [2011, 2013, and written communication, 2016] and *Singleton et al.* [2014a]. The two curved blue lines indicate detachment-fault displacement path based on the inference that the Harcuvar Mountains are a groove in the detachment-fault footwall. The segmented straight green lines indicate detachment-fault displacement path based on the inference that mylonitic lineations in the Buckskin and Rawhide Mountains record extension direction and that abundant right-lateral faults have distorted the grooves so that they appear more easterly oriented than mylonitic lineations but were originally aligned [*Singleton*, 2015]. Both displacement paths are based on the inference that the western Bouse Hills is the footwall cutoff for the base of Oligocene to lower Miocene strata with an equivalent hanging wall cutoff that is displaced to the axis of the Date Creek basin half graben. Breaks in the lines represent postdetachment strike-slip displacement, inferred to be substantial by *Singleton* [2015]. Note that the northern Plomosa Mountains detachment fault in the southwestern corner of the map area [*Spencer et al.*, 2014] projects below the Bouse Hills and the Harcuvar core complex. Basin-depth data are from *Richard et al.* [2007].

features indicate top-northeast displacement, with displacement of footwall rocks to the west-southwest out from beneath weakly extended crystalline rocks in central Arizona [e.g., *Reynolds and Spencer*, 1985; *Spencer and Reynolds*, 1989b; *Singleton and Mosher*, 2012]. Corrugations define six antiforms separated by synformal troughs. Corrugation axes are approximately parallel to mylonitic lineations in footwall rocks in the Harcuvar

Mountains, but lineation trend is oriented up to ~30° more northerly than the northeasterly trend of corrugation axes in the Rawhide, Buckskin, and Little Buckskin Mountains (Figure 2) [*Spencer et al.*, 1989a; *Bryant*, 1995; *Singleton*, 2011, 2013; *Singleton et al.*, 2014a]. Mylonitic fabrics are inferred to have formed downdip from the active detachment fault, as proposed by the shear-zone model for core complex genesis [*Davis et al.*, 1986]. The boundary between mylonitic and nonmylonitic footwall rocks, identified by the dashed line in Figure 2, is interpreted as an exhumed brittle-plastic transition where rocks to the southwest were in the brittle regime during initial extensional exhumation and were too cool for mylonitization.

Thermochronologic studies throughout the Harcuvar complex indicate sequential cooling from southwest to northeast or simply rapid mid-Miocene cooling. Emplacement of the 21–22 Ma Swansea plutonic suite in the Buckskin and Rawhide Mountains [*Bryant and Wooden*, 2008; *Singleton et al.*, 2014b] was followed by cooling through the argon-closure temperature for biotite in the western Buckskin Mountains at 17 Ma, the central and east-central Buckskin Mountains at 15 Ma, and the easternmost Buckskin Mountains at 12 Ma [*Spencer et al.*, 1989b; *Richard et al.*, 1990; *Bryant et al.*, 1991; *Scott et al.*, 1998]. (U-Th)-He dates are generally 1–3 Myr younger and show similar west-to-east cooling [*Brady*, 2002; *Singleton et al.*, 2014b]. The eastern, mylonitic tip of the Harquahala Mountains yielded six (U-Th)-He zircon dates at 15–16 Ma [*Prior et al.*, 2016], similar to three (U-Th)-He zircon dates of 15–17 Ma from mylonitic rocks in the southwestern Buckskin Mountains [*Singleton et al.*, 2014b]. Both these areas are near the southwestern limit of mylonitic footwall fabrics and so were at temperatures of mylonitization ($>$ ~300°C) when extension began and cooled below ~180°C [*Wolfe and Stockli*, 2010] at 15–17 Ma. Samples from the mylonitic eastern two thirds of the Harcuvar Mountains yielded (U-Th)-He apatite dates that indicate rapid low-temperature cooling at ~15 Ma [*Carter et al.*, 2004]. Fission-track apatite and zircon thermochronometers, as well as (U-Th)-He dates of crystalline hematite from hydrothermal mineral deposits associated with the detachment fault, have larger uncertainties but are consistent with the other thermochronometers [*Bryant et al.*, 1991; *Foster et al.*, 1993; *Evenson et al.*, 2014].

The western Bouse Hills west of the southern Buckskin Mountains include a southwest dipping sequence of sandstone, tuff, conglomerate, and limestone that rests on Proterozoic crystalline rocks [*Spencer and Reynolds*, 1990; *Spencer et al.*, 1995]. The basal depositional contact was interpreted as a footwall cutoff of the Buckskin-Rawhide detachment fault, with the equivalent hanging wall cutoff displaced ~68 km east-northeast to beneath Date Creek basin (Figure 2) [*Spencer and Reynolds*, 1991]. A (U-Th)-He thermochronologic profile from the western Bouse Hills northeastward into the southern Buckskin Mountains reveals early Cenozoic cooling in southwesternmost exposures probably due to gradual erosional exhumation, including a date of 64.5 ± 4.3 Ma from zircon [*Singleton et al.*, 2014b]. The western, nonmylonitic parts of the Harcuvar and Harquahala Mountains and the adjacent Granite Wash and Little Harquahala Mountains yielded (U-Th)-He apatite dates as old as 35 Ma and zircon dates as old as 55 Ma [*Carter et al.*, 2004; *Prior et al.*, 2016]. K-Ar and $^{40}Ar/^{39}Ar$ dates from mica also record preextension cooling history, with pre-60 Ma dates only from southwesternmost areas (Figure 2) [*Rehrig and Reynolds*, 1980; *Shafiqullah et al.*, 1980; *Reynolds et al.*, 1986; *Richard et al.*, 1990]. This cooling is probably due to erosional exhumation but might also reflect cooling from below due to shallow plate subduction and subduction-complex underplating [*Dumitru et al.*, 1991; *Haxel et al.*, 2015; *Strickland et al.*, 2016]. In either case, these dates record preextension thermal profiles that would be expected for the shallow-crustal breakaway zone of the detachment-fault system that exhumed the core complex.

In summary, top-northeast displacement of ~55–70 km uncovered the Harcuvar metamorphic core complex with an area of ~2000 km^2 of mylonitic footwall rock (excluding the Harquahala Mountains, which is largely nonmylonitic, and excluding McMullen Valley where a large tiltblock is present north of Aguila and more may be present in the deep basin beneath McMullen Valley; Figure 2). Tectonic restoration of a footwall cutoff at the base of west-tilted Oligocene-Miocene strata in the western Bouse Hills, to beneath the axis of Date Creek basin, is shown in Figure 2 (blue lines). The slightly arcuate restoration vectors parallel the crest of the Harcuvar Mountains. The arcuate path of the proposed extension vector is not unique, as a similar arcuate extension vector characterized exhumation of the Godzilla deep-sea core complex in the Philippine Sea [*Spencer and Ohara*, 2014]. An alternative restoration that places the western Bouse Hills beneath the Artillery Mountains (Figure 2, green line) is more consistent with mylonitic lineation trends in the Buckskin and Rawhide Mountains [*Singleton*, 2015] but is discordant to the Harcuvar groove and its mylonitic lineations. With a conservative estimate of 10 km preextension average depth to mylonitic footwall rocks, either

displacement path represents removal of ~20,000 km^3 of rock from above the complex with almost none remaining. The largest upper plate block of pre-Cenozoic rock remaining on the complex southeast of the Planet Peak antiform and northwest of the crest of the Harcuvar Mountains consists of approximate 1 km^3 in the Swansea mine area. The physics of such effective exhumation, characteristic of large continental and deep-sea core complexes, is poorly understood.

3. Structure of Upper Plate (Hanging Wall) Rocks

Upper plate rocks are better preserved in synformal corrugations than on antiforms within the Buckskin and Rawhide Mountains (Figure 3). Preserved rock units are diverse, including Proterozoic crystalline rocks, Paleozoic metasedimentary rocks, Mesozoic metavolcanic and metasedimentary rocks, and Oligocene to Miocene sedimentary and volcanic rocks and rock-avalanche breccias [e.g., *Reynolds and Spencer*, 1989]. The Oligocene to Miocene strata were deposited during extension within a basin or basins formed by extensional tectonism in a region that was previously a highland with no preextension Cenozoic sedimentary or volcanic rocks [*Spencer and Reynolds*, 1989a]. Pre-Cenozoic upper plate rocks are largely absent between the Planet Peak antiform and the crest of the Harcuvar Mountains, and most exposures consist of sedimentary and volcanic rocks deposited during extension. Syn-extension strata form a thick tilted sequence in the Artillery Mountains northeast of the Rawhide Mountains that was divided by *Lasky and Webber* [1949] into the Artillery Formation, Chapin Wash sandstone, and Sandtrap conglomerate (Figure 3). Some faulted upper plate strata in the Rawhide and Buckskin Mountains can be correlated with the units named by *Lasky and Webber* [1949] on the basis of lithologic similarity, but strict correlation is problematic because of thickness and facies changes [*Spencer and Reynolds*, 1989b]. As a result, the geologic maps presented here generally identify strata by lithology rather than by the unit names of *Lasky and Webber* [1949].

3.1. Maggie Wash Area

The area along lower Maggie Wash (formerly Sandtrap Wash) is at the tapered end of the extensional wedge northeast of the Rawhide Mountains (Figure 3, cross section A-A′; Figure 4). Conglomerate widely exposed in the area (Sandtrap conglomerate of *Lasky and Webber* [1949]) contains abundant clasts of mylonitic crystalline rocks and chloritic breccia derived from the mylonitic footwall [*Spencer et al.*, 2013]. It is the stratigraphically highest unit in a thick sequence of sedimentary and volcanic rocks with broadly fanning dips in cross section and the steepest dips at the lowest stratigraphic levels [*Yarnold*, 1994; *Lucchitta and Suneson*, 1993a; *Spencer et al.*, 1989c, 2013]. The stratigrapically lowest Artillery Formation includes basal arkose that rests on Proterozoic crystalline rocks, contains a 26.3 Ma tuff [*Lucchitta and Suneson*, 1993b], and dips ~40°–45° to the southwest (Figure 3, cross section A-A′) [*Spencer et al.*, 2013]. The arkosic sandstone grades up-section into siltstone and lacustrine limestone. The limestone is interbedded with, and overlain by, rock-avalanche breccias derived from metamorphic rocks like those displaced above the detachment fault along the northern margin of the core complex [*Yarnold*, 1994]. Volcanic and sedimentary rocks that overlie the limestone are in turn overlain by a widespread reddish sandstone unit (Chapin Wash Formation of *Lasky and Webber* [1949]). The reddish sandstone is overlain by, and grades upward into, the Sandtrap conglomerate, which is interbedded with a basalt dated at 9.6 ± 0.4 Ma [*Shafiqullah et al.*, 1980].

Folds are apparent in this stratal sequence in the lower Maggie Wash area, especially in the form of an anticline that extends for 3–4 km along the flank of the Rawhide Mountains in the footwall of the Sandtrap Wash fault (Figure 4). The west limb of the anticline is clearly cut off by the underlying detachment fault. As shown in the cross sections in Figure 4, the east limb is interpreted to be cut off by the detachment fault as well, but this is based on the assumption that the detachment fault does not greatly steepen downdip, but rather gently increases in dip over a 3–4 km distance away from the exposed trace of the detachment fault. The reddish sandstone unit is thicker to the northeast, as is apparent in cross section, and the anticline is interpreted as folding a section in which the conglomerate had prograded to the northeast over the sandstone and so is thinner to the northeast. The Sandtrap Wash fault appears to displace the top of the anticline 2–3 km to the northeast so that the two anticlines apparent in cross section were originally one.

Strata on the northeast limb of the anticline in the footwall of the Sandtrap Wash fault dip 15°–35° to the northeast and may be truncated by the detachment fault such that the detachment fault cuts up-section to the northeast. Northeast dips could be the result of tilting above a southwest dipping normal fault, except that no such fault is apparent from mapping northeast of the anticline (Figure 4) [*Spencer et al.*, 2013].

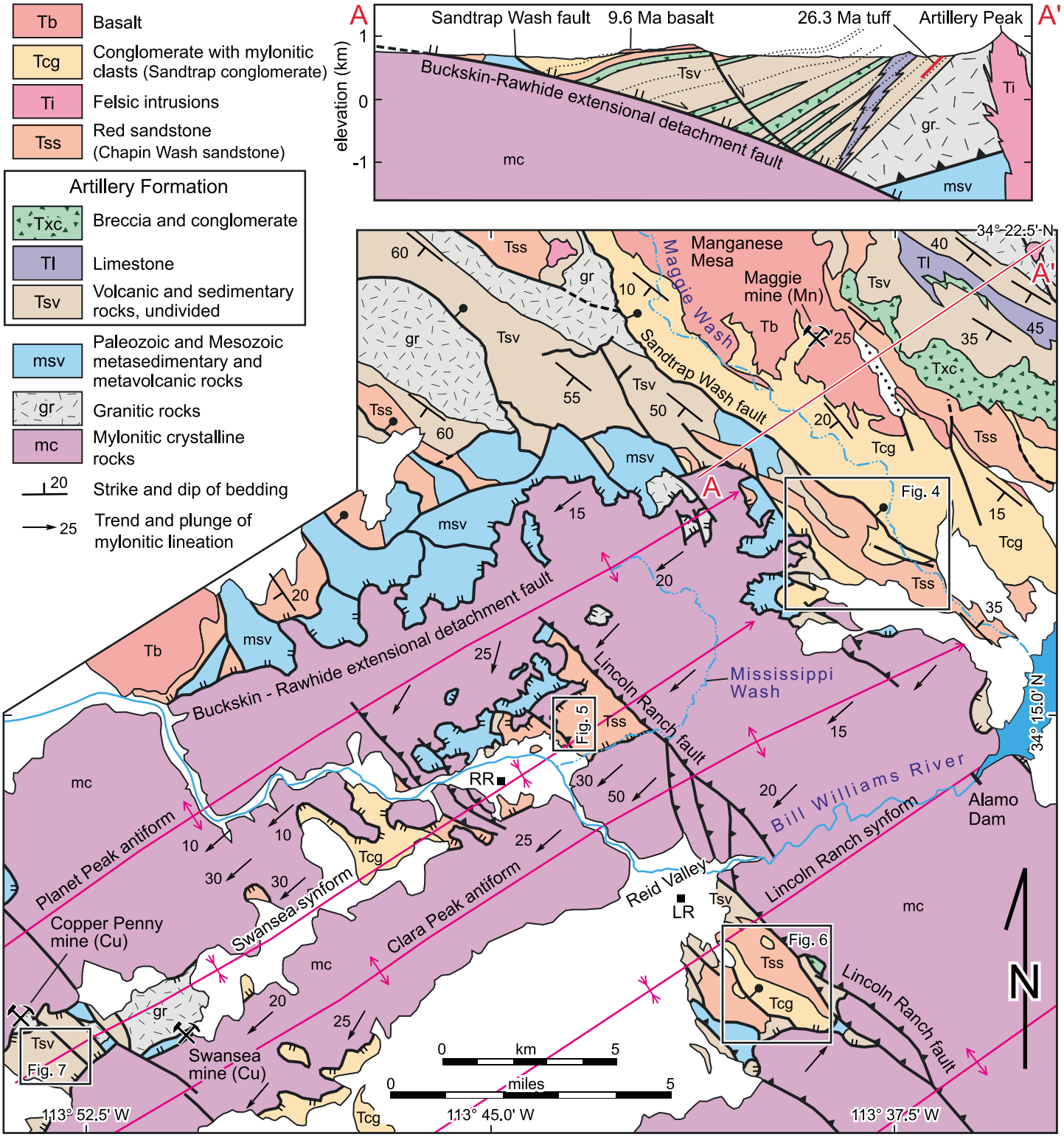

Figure 3. Geologic map and cross section of the northeastern Buckskin Mountains (the area south of the Bill Williams River), and the Rawhide and Artillery Mountains (the Artillery Mountains are northeast of Maggie Wash), showing locations of detailed map (Figures 4–7). Map data simplified from *Spencer* [1989], *Spencer and Reynolds* [1989b], *Shackelford* [1989], *Scott* [2004], *Lucchitta and Suneson* [1994], and *Spencer et al.* [2013]. See Figure 2 for location. LR = Lincoln Ranch; RR = Rankin Ranch.

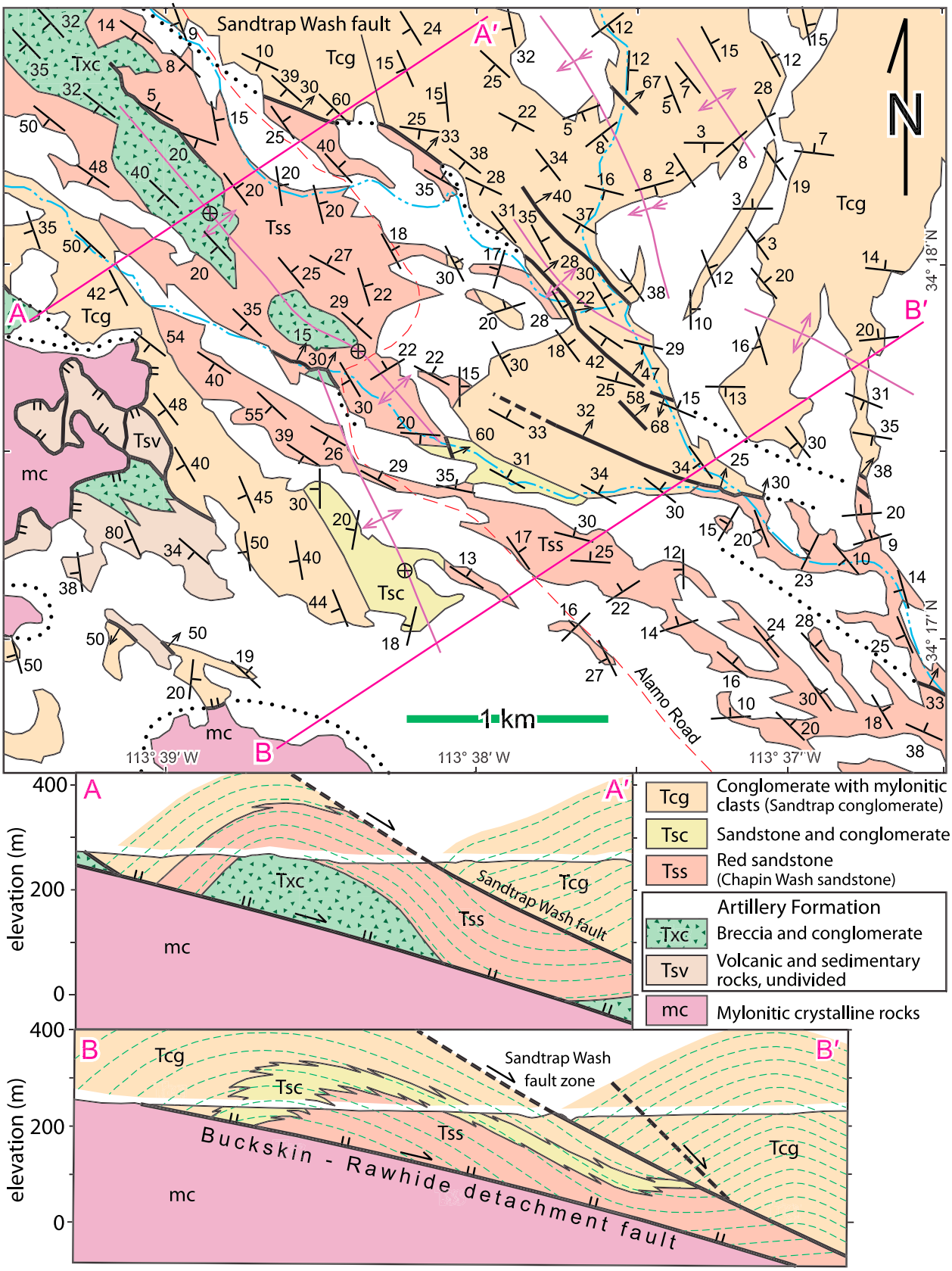

Figure 4. Geologic map and cross sections of the lower Maggie Wash area (simplified from *Spencer et al.* [2013]). See Figure 3 for location.

Alternatively, northeast bedding dips could be the result of a ramp-flat geometry in a northeast dipping normal fault that parallels bedding beneath the northeast dipping limb, but this would require the detachment fault to be as steeply northeast dipping as overlying beds. This would indicate significant steepening of the detachment fault (more so than shown on the cross sections), but is a possibility.

3.2. Mississippi Wash Area

Strata in the lower Mississippi Wash area in the southern Rawhide Mountains (Figure 3) consist largely of arkosic sandstone and conglomeratic sandstone that are similar to the reddish sandstone mapped farther east in the Artillery Mountains (Figure 5) [*Scott and Lister*, 1992; *Scott*, 1995, 2004]. The strata contain a bed of poorly lithified silicic tuff that serves as a marker bed and are folded with northeast-dipping beds on the northeast side of two anticlines (Figure 5). Farther east of one of the anticlines are two southwest dipping normal faults that could be responsible for the northeast tilting (cross sections A and C on Figure 5), but the northeast-dipping limb of the other, southern anticline is not flanked by any mapped normal fault (cross section B on Figure 5). It is possible that northeast tilting occurred above one or more concealed, southwest dipping normal faults, although such faults are not apparent to the north of cross section B (Figure 5) where they would likely strike toward the northeast end of the cross section.

3.3. Reid Valley Area

Most exposed upper plate rocks southeast of Reid Valley in the eastern Buckskin Mountains (Figure 3) consist of reddish sandstone and tan conglomerate containing 30–40% to perhaps as high as 65% mylonitic and chloritic breccia clasts [*Spencer and Reynolds*, 1989b; *Prior and Singleton*, 2016]. The detachment fault projects at a gentle angle beneath the strata, and a small window into the detachment fault is present on the south flank of the basin (Figure 6) [*Spencer and Reynolds*, 1989b; *Singleton et al.*, 2014a]. The sandstone and conglomerate are folded into an anticline bounded on the southwest by a northeast dipping normal fault and on the northeast by a syncline (cross section A-A′) and by the Lincoln Ranch fault (cross section B-B′), a northwest striking fault with reverse and right-lateral strike-slip displacement [*Spencer and Reynolds*, 1989b; *Singleton*, 2015]. Farther north in the Rawhide Mountains, the Lincoln Ranch fault cuts postdetachment strata, indicating that it is significantly younger than displacement on the detachment fault [*Scott*, 2004].

Cross sections through the anticline indicate that it is truncated by the underlying detachment fault unless the fault itself is strongly folded in a way that is not apparent from the nearby fault trace. As with the areas described previously, the detachment fault appears to cut up-section to the northeast beneath the northeast dipping limb of the anticline. This would be consistent with a southwest dipping normal fault to the northeast and tilting above such a fault, but no fault with this displacement was identified. It is possible that such a fault was present farther northeast and was elevated and eroded away in the hanging wall of the Lincoln Ranch reverse fault. Alternatively, the strata are simply folded and the folds are truncated by postfolding displacement on a gently to moderately northeast dipping normal fault that displaced the folded rocks downward into contact with the detachment-fault footwall.

3.4. Copper Penny Mine Area

The Copper Penny mine area is located near the southwestern end of the Swanea synform (Figure 3). A thick sequence of sedimentary and volcanic rocks and rock-avalanche breccia in this area is folded into a southeast plunging anticline, with limbs that dip up to 80° (Figure 7) [*Wilkins and Heidrick*, 1982; *Spencer and Reynolds*, 1989b]. If the southeast plunging axis of the main anticline were restored to horizontal, a fault zone on the west flank of the anticline would have the dip and displacement of a normal fault. The anticline is bounded to the northeast by what appears to be a steep, northeast dipping normal fault with another anticline to the northeast. It is possible that this northeastern anticline is the displaced top of the anticline to the southwest. The northeastern anticline is bounded to the northeast by a southwest dipping normal fault with Proterozoic granitic rocks in its footwall (northeast end of cross section A-A′ in Figure 7).

4. Interpretation

Folding of syntectonic strata, and truncation of folds by the underlying Buckskin-Rawhide detachment fault, is characteristic of the extensional basin or basins that formed in the study areas. All of the major folds described have axes approximately perpendicular to regional extension direction, with interlimb angles of

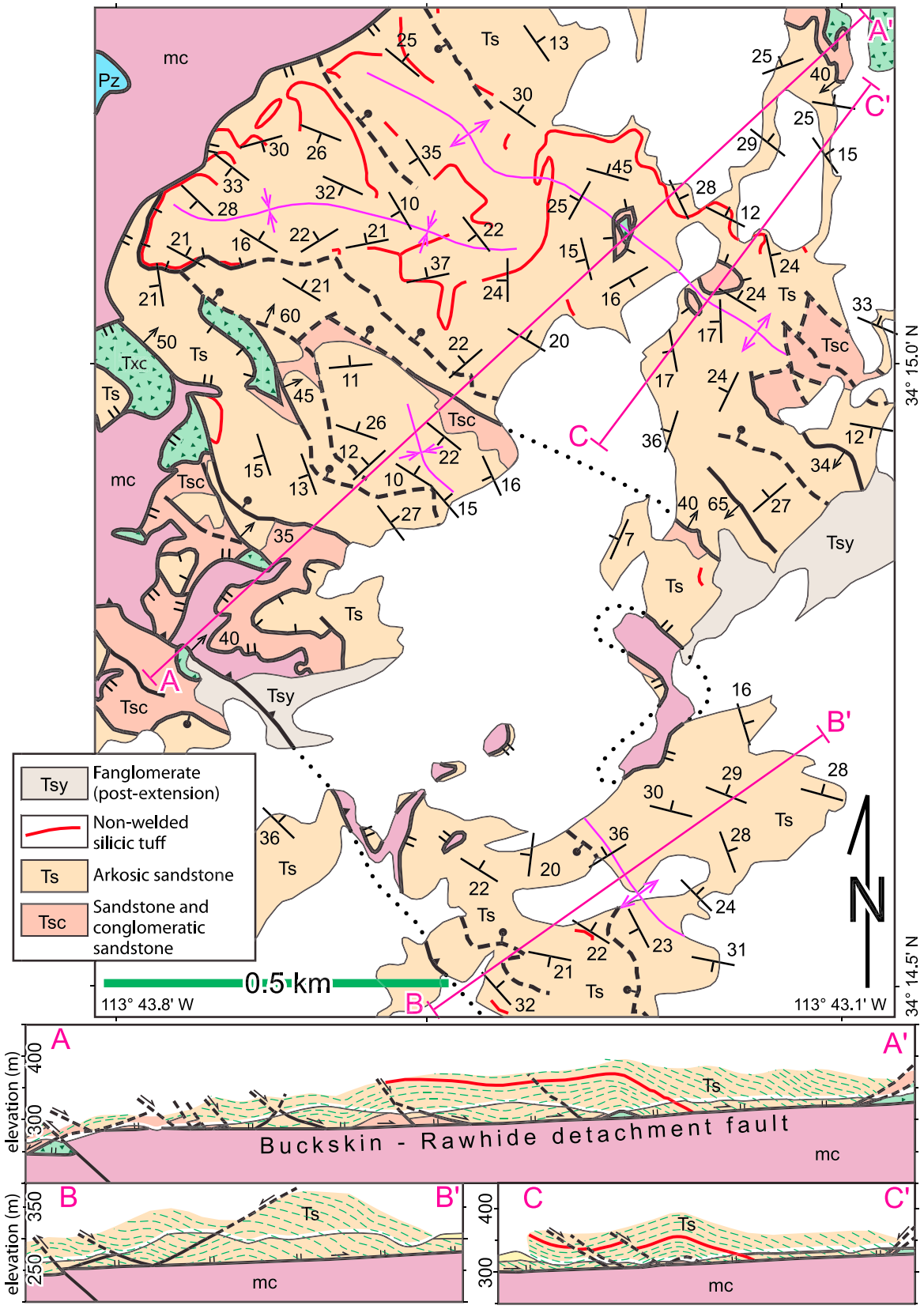

Figure 5. Geologic map and cross sections of part of the southern Rawhide Mountains near lower Mississippi Wash (simplified from plates 4 and 5 of *Scott* [2004]). Txc = breccia and conglomerate; Pz = Paleozoic metasedimentary rocks; mc = mylonitic crystalline rocks. See Figure 3 for location.

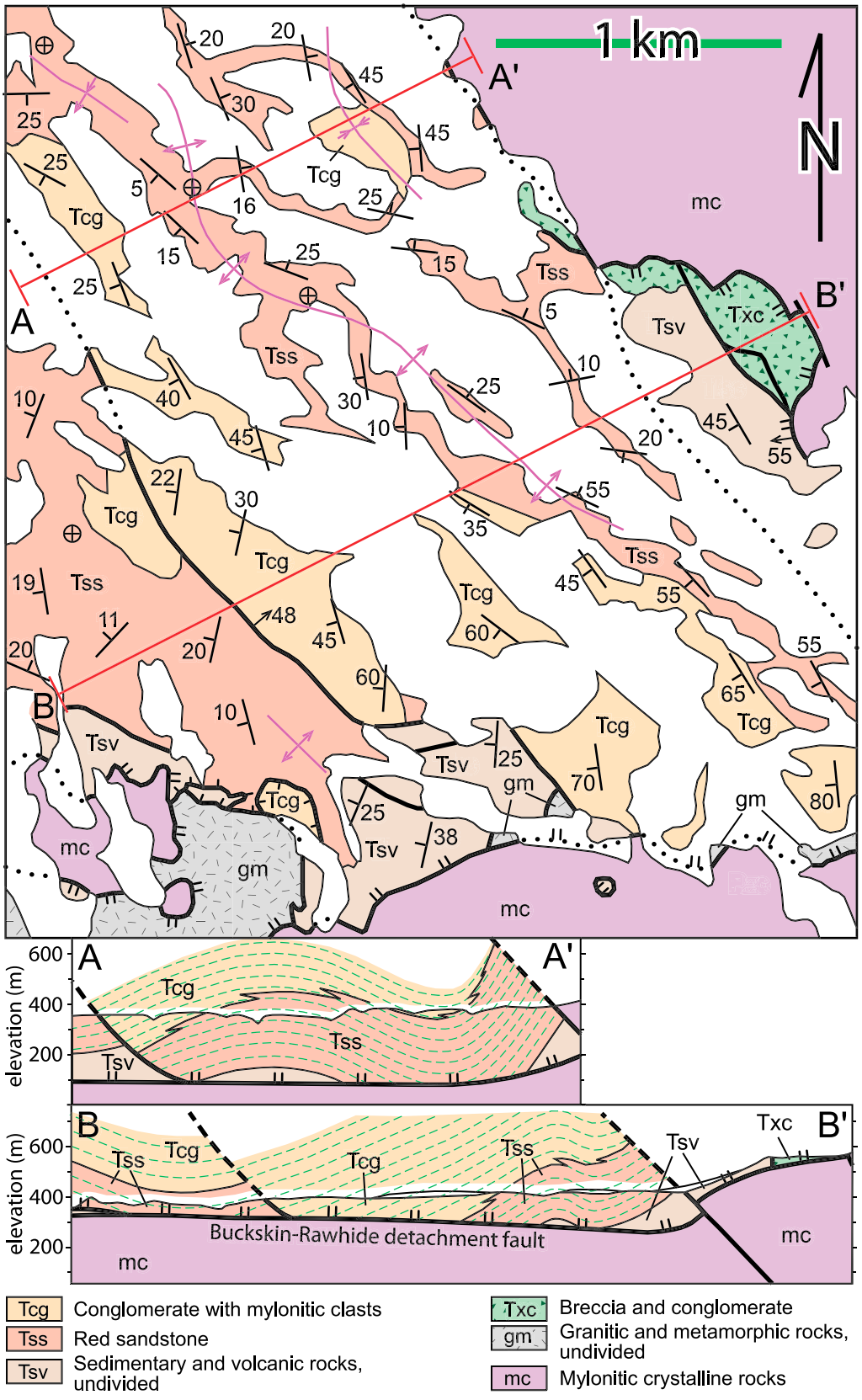

Figure 6. Geologic map and cross sections of the southeastern Reid Valley area in the eastern Buckskin Mountains (simplified from *Spencer and Reynolds* [1989b]). See Figure 3 for location.

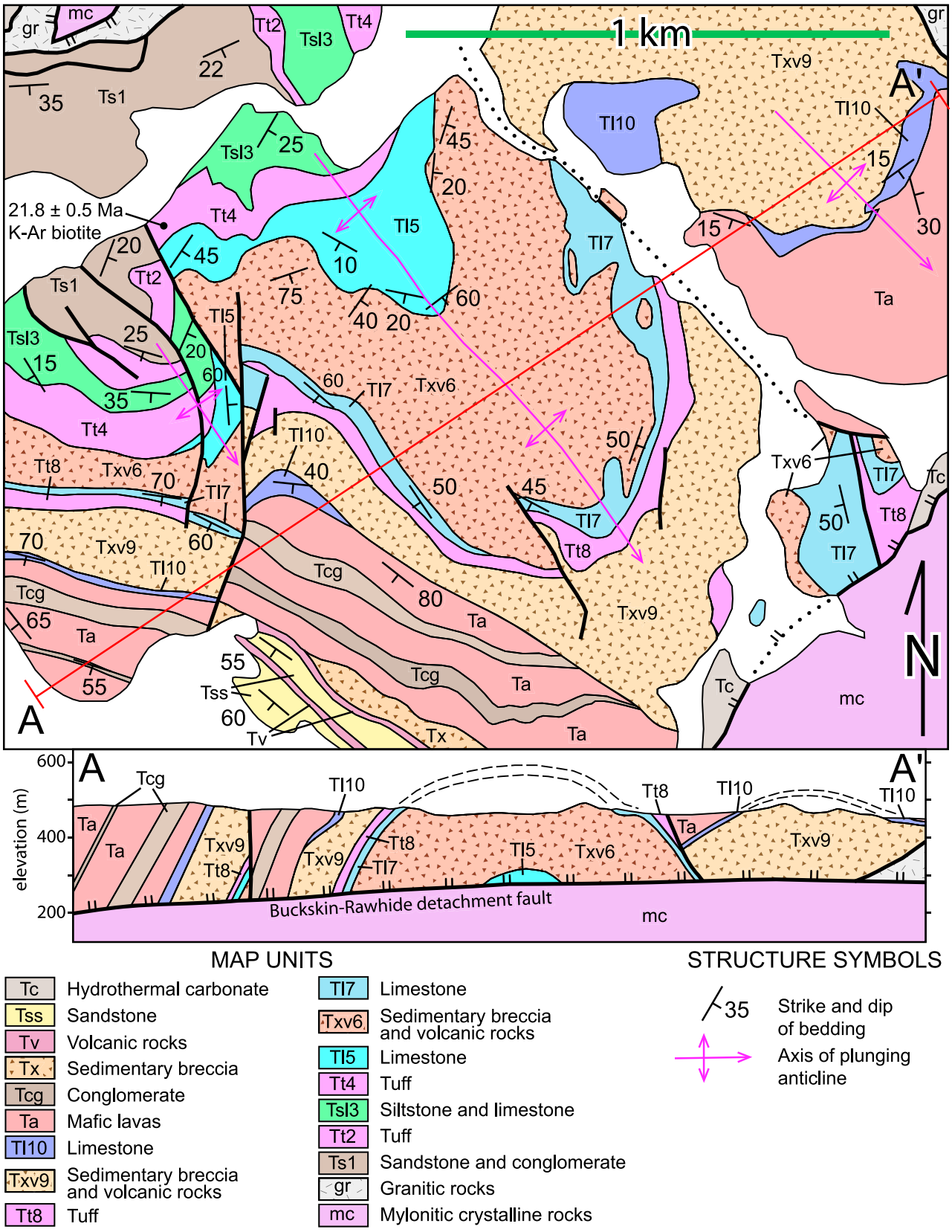

Figure 7. Geologic map and cross sections of the Copper Penny mine area in the central Buckskin Mountains (simplified from *Spencer and Reynolds* [1989b]). See Figure 3 for location.

~80°–140°. Minor folds, including both synclines and anticlines, are generally more open but similarly oriented. Tilting and warping of strata above listric normal faults are common in extensional basins, with beds dipping toward the breakaway [e.g., *Xiao and Suppe*, 1992; *Schlische*, 1995; *Janecke et al.*, 1998]. A less common feature, characteristic of anticlines in all four study areas, is that the northeast anticline limbs dip northeastward into the underlying, top-northeast detachment fault. This would be expected for fault-propagation folds that produce monoclinal flexures with dips toward the hanging wall side of the underlying normal fault [e.g., *Grasemann et al.*, 2005]. Anticlines like those in the study areas could conceivably result from fault-propagation folding followed by tilting to the southwest above younger, northeast dipping normal faults. This explanation is difficult to reconcile, however, with the absence of normal faults near the axial planes of the anticlines, the abundance of minor folds, and the absence of any demonstrable extensional, fault-propagation folds in the region.

Another possibility is that folding was a consequence of displacement above northeast dipping normal faults with ramp-flat geometry. A problem with this interpretation is that it would require normal faults to cut up-section to the northeast, which would be geometrically and mechanically difficult, especially where strata were previously tilted to the southwest. In some cases anticlines could be interpreted as the result of displacement on dual listric normal faults that dip inward toward the anticline axial plane. A problem with this interpretation is that southwest dipping normal faults are demonstrably absent northeast of the anticline axis in the Maggie Wash area and appear to be absent in the Reid Valley area. There are enough problems with the various fold mechanisms outlined above that we consider an alternative hypothesis that the folds are a consequence of simple shortening within an extensional wedge, with shortening occurring before a final period of extension that dismembered the folds.

4.1. Critical-Taper Theory

Application of critical-taper theory (also known as critical Coulomb wedge theory) to problems of tectonics is based on the concept that thrust belts, accretionary wedges, and extensional wedges are sufficiently lacking in mechanical cohesion that they can be modeled as cohesiveless materials at scales of ~10^2–10^5 m. Cohesiveless materials, such as dry sand, have frictional resistance to slip and can support slopes up to an angle of repose. In this case, there is no true tension and no tensional side of a Mohr circle diagram, which greatly simplifies quantitative representation of material properties and allows an exact analytical representation of wedge behavior [*Dahlen*, 1984]. Critical-taper theory represents wedges of cohesionless material in extensional and shortening settings in which frictional resistance to slip on a basal slip surface is less than the frictional resistance to slip within the wedge. In this situation stable sliding of the wedge is possible if fault dip and surface slope are within the stable-sliding field for wedge parameters (Figures 8 and 9) [*Dahlen*, 1984].

First-motion and moment-tensor interpretations of earthquakes in actively extending areas indicate that almost all normal faults have fault dips of $>$30° at depths of earthquake initiation and for the geometry of total seismic-energy release [*Jackson and White*, 1989]. A small number of normal-fault earthquakes have been identified with dips in the range of 15°–30° [*Abers*, 1991; *Hreinsdóttir and Bennett*, 2009] or even less, especially for segments of irregular faults [e.g., *Mirabella et al.*, 2011]. The stability field outlined in black in Figure 9 allows for fault dips as low as 20° to accommodate these rare earthquakes. Shown in red in Figure 9 is the stable-sliding field that encloses fault-ramp and surface-slope measurements of some large Quaternary core complexes that appear to have been completely denuded by stable sliding, including the Pompangeo and Tokorondo complexes in central Sulawesi, Indonesia, the Gurla Mandhata core complex in the Himalaya, and Dayman dome in Papua New Guinea [*Murphy et al.*, 2002; *Daczko et al.*, 2009, 2011; *Spencer*, 2010, 2011]. This empirically determined stable-sliding field allows for a theoretical minimum dip of 3° for extensional detachment faults (at zero taper) [*Spencer*, 2011]. Similar extensional-wedge parameters for stable sliding during continental breakup were identified based on marine seismic data [*Nirrengarten et al.*, 2016].

The large discrepancy between minimum fault dip associated with earthquakes and the much lower dip of fault ramps on the flanks of many core complexes is poorly understood. It is possibly due to fault curvature in cross section such that only the shallowest part of the fault is gently dipping and this part of the fault is neither the site of earthquake initiation nor responsible for a large fraction of total seismic energy release [*Spencer*, 2011]. Although consistent with the rolling-hinge model for core-complex exhumation [*Wernicke and Axen*, 1988; *Buck*, 1988], such fault curvature does not explain why slip occurs on the gently dipping part

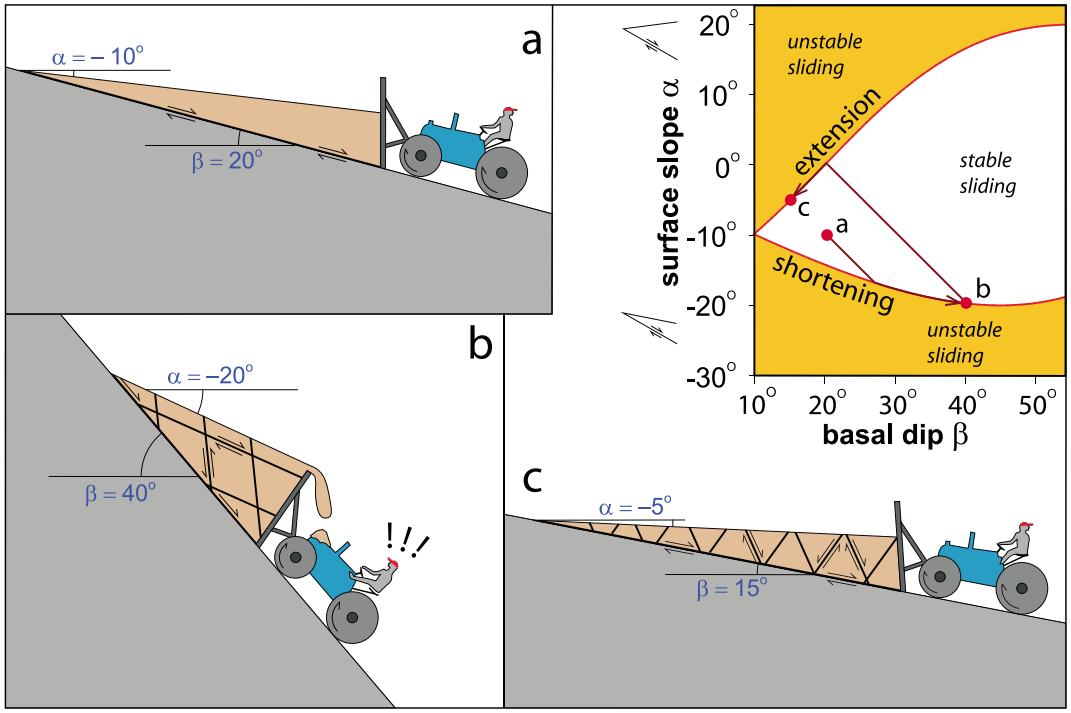

Figure 8. Extensional-wedge behavior illustrated by a hypothetical tractor backing down hill with a wedge of dry (noncohesive) sand on an icy (low friction) slope (inspired by *Xiao et al.* [1991]). Stable-sliding field for wedge, and points representing frames a, b, and c, are shown in upper right. (a) Stable sliding at point a. (b) As hill becomes steeper, both hillslope (basal-slip angle) and wedge-surface slope change until the margin of the stable-sliding field is reached and wedge shortening begins. Point b in upper right indicates wedge parameters when basal-slip angle reaches 40°. (c) As hillslope becomes gentler, both basal-slip angle and surface slope change until the margin of the stable-sliding field is reached and wedge extension begins. Point c in upper right indicates wedge parameters when basal slip angle reaches 15°. Slip surfaces within wedge are shown to illustrate deformation, but critical-taper theory is based on the inference that wedge deformation occurs simultaneously at all points in the mechanically homogeneous wedge [*Dahlen*, 1984].

of the fault beneath the tapered wedge tip when the wedge tip could be transferred to the footwall by extensional dismemberment.

4.2. Application of Critical-Taper Theory to Folding in the Buckskin-Rawhide-Artillery Mountains

We use a critical-taper stability field with a 3° theoretical minimum fault dip (at zero taper), as appropriate for Quaternary metamorphic core complexes with highly effective tectonic exhumation [*Spencer*, 2011], to evaluate the possibility of a state of stress leading to shortening in the extensional wedge above the Buckskin-Rawhide detachment fault (Figure 10). We make the assumption that as the dip of the basal arkose in the Artillery Mountains increased during extension, the dip of detachment fault beneath the extensional wedge decreased at the same rate. This assumption would be inappropriate if significant amounts of upper plate rock were displaced as slivers from beneath the wedge and transferred to the lower plate, which could cause tilting without ultimately changing detachment-fault dip, but the highly effective exhumation of footwall rocks in the Buckskin and Rawhide Mountains justifies the assumption in this case, at least for deeper parts of the wedge (the basal arkose and underlying bedrock). We assume, furthermore, that the detachment fault was broadly listric in its original cross-sectional form and that southwestward tilting of the wedge was accommodated within the wedge by normal faults north and east of Artillery Peak [*Bryant*, 1995; *Spencer et al.*, 2013]. More than about 5–8 km northeast of Artillery Peak, normal faults are sparse and small, the upper plate is largely unmodified by extension [*Bryant*, 1992; *Spencer and Reynolds*, 1991] (Figure 6), and the dip of the underlying detachment fault and its down-dip continuation as a ductile shear zone did not obviously change during extension.

Erosion and sedimentation during tilting generally would reduce surface slope, while sedimentation would extend the wedge tip with progressively lower taper. As a result of erosion and sedimentation, the extensional

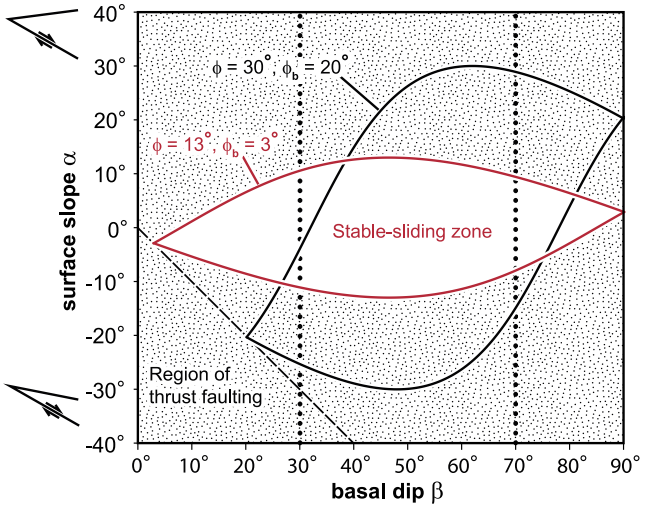

Figure 9. Two stable-sliding zones with different parameters. The dotted lines bound a basal slip range of 30°–70°, as determined by evaluation of normal-fault dip from earthquake seismology [*Jackson and White*, 1989]. The black solid lines outline stable-sliding region for a maximum surface slope φ of 30° and minimum basal slip angle φ_b of 20°. This would allow for normal-fault earthquakes on faults dipping as little as 20° [e.g., *Abers*, 1991]. The red lines outline stable-sliding region for a maximum surface slope φ of 13° and minimum basal slip angle φ_b of 3° as determined from fault ramps adjacent to Quaternary detachment faults associated with terrestrial and submarine core complexes [*Spencer*, 2010, 2011] and is similar to that for submarine extensional wedges associated with continental rifting and breakup [*Nirrengarten et al.*, 2016].

margin of the wedge stability field is reached with a surface slope near horizontal and a detachment-fault dip of 5°–10° (Figure 10, location 7). We infer that transfer of slivers of primarily sedimentary rocks from the tapered end of the wedge to the lower plate occurred under these conditions.

Because the critical-taper stability field represents the tapered end of core-complex wedges with a 3° minimum fault dip, a point representing wedge parameters could migrate to the shortening side of the wedge-stability field if an alluvial fan builds onto the wedge from the core complex. This is not true for minimum fault dips of greater than ~8°–12°. As shown in Figure 10 (location 9), alluvial fans with surface slopes of ~4°–7° will move the wedge to the shortening side of the stable-sliding field above a detachment fault with a fault dip of ~4°–15°. This raises the possibility that wedge shortening in the Buckskin-Rawhide-Artillery Mountains was triggered by core-complex emergence and development of alluvial fans with surface slopes away from the core complex. The distribution of folded strata also allows for the possibility that alluvial-fan apexes were located in synformal detachment-fault grooves and that shortening occurred preferentially in these areas (core-complex wedgies) because fault dip was less and surface slope was greater near fan apexes. It is also possible that tilting of the entire wedge away from the rising and arching core complex triggered shortening by increasing both surface slope and fault dip in the direction away from the core complex (as in Figure 9b). This could have occurred during erosion of the wedge without alluvial-fan development, provided that erosion was not sufficient to reduce surface slope to the point of preventing the wedge from reaching the shortening margin of the stable-sliding field.

We interpret cross sections of folded rocks in the Mississippi Wash, Reid Valley, and Copper Penny mine areas as representing folds that were cut by normal faults, with the hanging wall rocks of these normal faults then displaced into contact with mylonitic crystalline rocks that make up the lower plate. This was followed by deactivation of the directly underlying normal fault as the breakaway fault stepped northeastward, leaving stranded fragments of hanging wall rock resting on what is mapped as the Buckskin-Rawhide detachment fault. Initiation and movement on the Sandtrap Wash fault also appear to represent transfer of folded strata to the lower plate during the last increment of detachment-fault movement.

Theoretically, unstable sliding on the extensional margin of the critical-taper stability field can proceed until the wedge has zero taper and infinite length. In reality, however, wedge strength is not homogeneous and individual normal faults provide weak zones that accommodate wedge extension. Transfer of shortened rocks to the lower plate by extensional dismemberment requires displacement of the wedge configuration from the shortening side of the wedge-stability field where folding occurred (Figure 10, location 9), through the stable-sliding region, to the extensional side of the stability field where extensional dismemberment occurred (Figure 10, location 10). This change from shortening to extensional stress conditions could have resulted from a reduction in surface slope due to erosion, a reduction in detachment-fault dip due to tectonic processes, or both. The fact that this change occurred for multiple fault slivers in two different detachment-fault synforms suggests that stress conditions in the extensional wedge were close to the left

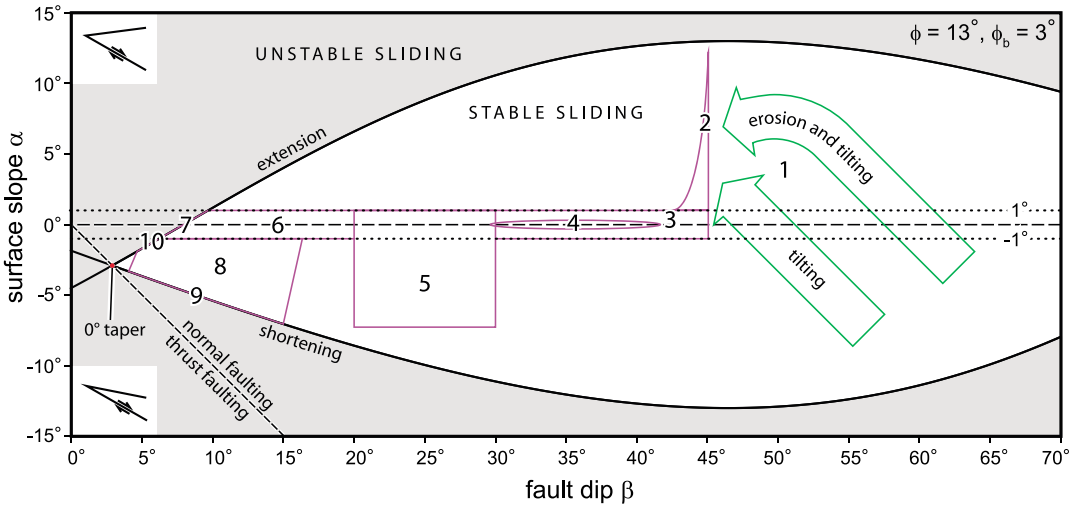

Figure 10. Proposed evolution of the trailing edge of the extensional wedge above the Buckskin-Rawhide extensional detachment fault. Note that many of the 10 critical-taper-parameter regions represent wedge behavior following addition of new material to the wedge tip. Numbers represent wedge-tip critical-taper settings, as follows: (1) Tilting and erosion of crystalline rocks during initial tilting above a normal fault that would evolve to form the Buckskin-Rawhide detachment fault. This is hypothetical because there is no actual record of this tilting. (2) Deposition of the basal arkose derived from the northeast, including basal conglomerate, which now dips ~40°–45° near Artillery Peak (Figure 3). (3) Deposition of sandstone and siltstone with surface slope of less than 1°. (4) Deposition of limestone with an approximately horizontal slope. (5) Deposition of conglomerate, sandstone, basalt flows, and rock-avalanche breccia with likely western or northwestern sources. It is possible that deposition of lavas and breccias created surface slopes adequate to trigger shortening, but the strata in this part of the stratigraphic section are so disrupted that evidence of shortening, if it exists, is obscure. (6) Deposition of reddish sandstone (Chapin Wash Formation of *Lasky and Webber* [1949]), with continued tilting until (7) extensional dismemberment of the wedge tip transfers slivers of the wedge to the footwall (this would apply to fault slivers that are not folded). (8) Alluvial-fan construction onto the reddish sandstone unit displaces wedge-tip setting through the stable-sliding region to (9) where folding occurs during unstable sliding at the shortening margin of the stable-sliding field. (10) Wedge-tip setting returns to unstable sliding in extension so that folded rocks in the wedge tip are transferred to the footwall by extensional dismemberment.

tip of the stable-sliding field for deformation within the wedge. In this situation, small changes in surface slope and/or detachment-fault dip could have resulted in ~90° rotation of the principal stresses associated with deformation. Indeed, the complex and multiple periods of deformation recognized in some extensional wedges [e.g., *Scott and Lister*, 1992] are consistent with multiple large changes in stress conditions.

Finally, we note that wedge shortening above a normal fault promotes core-complex exhumation. During shortening, the rate of displacement at the wedge tip is greater than the displacement rate farther down the underlying detachment fault. This will have the effect of accentuating effective exhumation which would, in turn, promote isostatic uplift of the footwall, thereby promoting more wedge shortening. This effect is likely to be minor, however, given the thinness of the wedge tip where folding occurred.

5. Conclusion

The Harcuvar metamorphic core complex underwent highly effective tectonic exhumation during Oligocene-Miocene tectonic extension, resulting in nearly complete removal of pre-Cenozoic basement from above much of the core complex. Exhumation was associated with erosion of lower plate mylonitic rocks and dispersal of mylonitic clasts to the extensional basin flanking the emerging core complex. Several conclusions derived from detailed geologic mapping of upper plate strata in the Buckskin-Rawhide-Artillery Mountains are as follows:

1. Oligocene-Miocene strata forming part of the upper plate of the core complex are strongly folded in four locations, with fold axes approximately perpendicular to regional extension direction. The folds affect entire syn-tectonic stratigraphic sections, but the folds are truncated by the underlying extensional detachment fault, demonstrating that folding occurred late during the period of tectonic extension.

2. Various causes of folding identified in other areas of extension, including displacement over one or more normal faults with curved or ramp-flat geometry, may have produced folds in the study area. Because of difficulties in accounting for some of the larger folds by these mechanisms, and the abundance of folds, we consider the possibility that the folds represent simple shortening in an extensional wedge.
3. To evaluate stresses that might have caused shortening, we apply critical-taper theory to an extensional wedge above a normal fault with so little friction that sliding can occur at a theoretical minimum dip of 3°. This approach is justified by gentle detachment-fault dips at the foot of several Quaternary core complexes characterized by highly effective core-complex exhumation [*Spencer*, 2011] and by the gentle dips below some submarine extensional wedges as identified by seismic reflection profiles [*Nirrengarten et al.*, 2016]. This evaluation leads to the conclusion that shortening in the wedge will occur if surface slope is inclined sufficiently away from the core complex.
4. Because of the accessibility of the shortening side of the critical-taper stability field for an extensional wedge with low basal friction, we conclude that a rising core complex can cause folding and shortening by tilting the wedge away from the rising core complex, development of an alluvial-fan emanating from the core complex, or both. A sedimentary trigger for folding is consistent with alluvial-fan deposits forming the youngest strata in folded sections in two of the four areas of folding described in this study.
5. In a tectonic setting of wedge shortening, detachment-fault displacement would occur at a greater rate near the wedge tip than farther down the detachment fault. Although stable sliding alone is sufficient for core-complex exhumation, wedge shortening will enhance effective exhumation and might even have a minor effect in promoting isostatic uplift and further wedge shortening.

Acknowledgments

The four geologic maps and associated cross sections that are the basis for this report are derived from published and cited geologic maps available from the Arizona Geological Survey (http://www.azgs.az.gov/) Document Repository (http://repository.azgs.az.gov/). We thank Brian Wernicke and Gianreto Manatschal for thoughtful reviews that improved clarity and focus. R. Scott gratefully acknowledges financial support from a Commonwealth Postgraduate Research Award. He also thank Gordon Lister for his enthusiasm and engagement in this project and Wayne and Sheree Pitrat for their hospitality, including allowing use of their cabin at Rankin Ranch in the Buckskin Mountains. Field mapping by J. Spencer in the Artillery and Rawhide Mountains in 2011–2012 was supported by the U.S. Geological Survey National Cooperative Geologic Mapping Program under STATEMAP assistance award G11AC20455. The views and conclusions contained in this document are those of the authors and should not be interpreted as necessarily representing the official policies, either expressed or implied, of the U.S. Government. This manuscript is submitted for publication with the understanding that the United States Government is authorized to reproduce and distribute reprints for governmental use.

References

Abers, G. A. (1991), Possible seismogenic shallow-dipping normal faults in the Woodlark-D'Entrecasteaux extensional province, Papua New Guinea, *Geology*, *19*(12), 1205–1208, doi:10.1130/0091-7613(1991)019<1205:PSSDNF>2.3.CO;2.

Brady, R. J. (2002), Very high slip rates on continental extensional faults: New evidence from (U-Th)/He thermochronometry of the Buckskin Mountains, Arizona, *Earth Planet. Sci. Lett.*, *197*(1–2), 95–104, doi:10.1016/S0012-821X(02)00460-0.

Brandes, C., and D. C. Tanner (2014), Fault-related folding: A review of kinematic models and their application, *Earth Sci. Rev.*, *138*, 352–370, doi:10.1016/j.earscirev.2014.06.008.

Bryant, B. (1992), Geologic map of the Poachie Range, Mohave and Yavapai counties, Arizona: *U.S. Geological Survey Misc. Investigations Map*, I-2198, scale 1:25,000.

Bryant, B. (1995), Geologic map, cross-sections, isotopic dates, and mineral deposits of the Alamo Lake 30′ × 60′ quadrangle, west-central Arizona, *U.S. Geological Survey Misc. Investigations Map*, I-2489, 3 sheets, scale 1:100,000.

Bryant, B., and J. L. Wooden (2008), Geology of the northern part of the Harcuvar complex, west-central Arizona, *U.S. Geological Survey Prof. Pap.*, 1752, 52 p.

Bryant, B., C. W. Naeser, and J. E. Fryxell (1991), Implications of low-temperature cooling history on a transect across the Colorado Plateau-Basin and Range boundary, west central Arizona, *J. Geophys. Res.*, *96*(B7), 12,375–12,388, doi:10.1029/90JB02027.

Buck, W. R. (1988), Flexural rotation of normal faults, *Tectonics*, *7*(5), 959–973, doi:10.1029/TC007i005p00959.

Carter, T. J., B. P. Kohn, D. A. Foster, and A. J. W. Gleadow (2004), How the Harcuvar Mountains metamorphic core complex became cool: Evidence from apatite (U-Th)/He thermochronology, *Geology*, *32*(11), 985–988, doi:10.1130/G20936.1.

Daczko, N. R., P. Caffi, J. A. Halpin, and P. Mann (2009), Exhumation of the Dayman dome metamorphic core complex, eastern Papua New Guinea, *J. Metamorph. Geol.*, *27*, 405–422, doi:10.1111/j.1525-1314.2009.00825.x.

Daczko, N. R., P. Caffi, and P. Mann (2011), Structural evolution of the Dayman dome metamorphic core complex, eastern Papua New Guinea, *Geol. Soc. Am. Bull.*, *123*(11/12), 2335–2351, doi:10.1130/B30326.1.

Dahlen, F. A. (1984), Noncohesive critical Coulomb wedges: An exact solution, *J. Geophys. Res.*, *89*(B12), 10,125–10,133, doi:10.1029/JB089iB12p10125.

Davis, G. A., and G. S. Lister (1988), Detachment faulting in continental extension: Perspectives from the southwestern U.S. Cordillera, in *Processes in Continental Lithosphere Deformation*, *Geol. Soc. Am. Spec. Pap.*, vol. 218, edited by S. P. Clark Jr., B. C. Burchfiel, and J. Suppe, pp. 133–160, Boulder, Colo., doi:10.1130/SPE218-p133

Davis, G. A., G. S. Lister, and S. J. Reynolds (1986), Structural evolution of the Whipple and South Mountains shear zones, southwestern United States, *Geology*, *14*, 7–10, doi:10.1130/0091-7613(1986)14<7:SEOTWA>2.0.CO;2.

Dumitru, T. A., P. B. Gans, D. A. Foster, and E. L. Miller (1991), Refrigeration of the western Cordilleran lithosphere during Laramide shallow-angle subduction, *Geology*, *19*(11), 1145–1148, doi:10.1130/0091-7613(1991)019<1145:ROTWCL>2.3.CO;2.

Evenson, N. S., P. W. Reiners, J. E. Spencer, and D. L. Shuster (2014), Hematite and Mn oxide (U-Th)/He dates from the Buckskin-Rawhide detachment system, western Arizona: Gaining insights into hematite (U-Th)/He systematics, *Am. J. Sci.*, *314*, 1373–1435, doi:10.2475/10.2014.01.

Foster, D. A., A. J. W. Gleadow, S. J. Reynolds, and P. G. Fitzgerald (1993), Denudation of metamorphic core complexes and the reconstruction of the Transition Zone, west central Arizona: Constraints from apatite fission track thermochronology, *J. Geophys. Res.*, *98*(B2), 2167–2186, doi:10.1029/92JB02407.

Grasemann, B., S. Martel, and C. Passchier (2005), Reverse and normal drag along a fault, *J. Struct. Geol.*, *27*(6), 999–1010, doi:10.1016/j.jsg.2005.04.006.

Haxel, G. B., C. E. Jacobson, and J. H. Wittke (2015), Mantle peridotite in newly discovered far-inland subduction complex, southwest Arizona: Initial report, *Int. Geol. Rev.*, *57*(5–8), 871–892, doi:10.1080/00206814.2014.928916.

Howard, K. A., and B. E. John (1987), Crustal extension along a rooted system of imbricate low-angle faults: Colorado River extensional corridor, California and Arizona, in *Continental Extensional Tectonics*, edited by M. P. Coward, J. F. Dewey, and P. L. Hancock, *Geol. Soc. London, Spec. Publ.*, *28*, 299–311.

Hreinsdóttir, S., and R. A. Bennett (2009), Active aseismic creep on the Alto Tiberina low-angle normal fault, Italy, *Geology*, *37*(8), 683–686, doi:10.1130/G30194A.1.

Jackson, J. A., and N. J. White (1989), Normal faulting in the upper continental crust: Observations from regions of active extension, *J. Struct. Geol.*, *11*(1–2), 15–36, doi:10.1016/0191-8141(89)90033-3.

Janecke, S. U., C. J. Vandenburg, and J. J. Blankenau (1998), Geometry, mechanisms, and significance of extensional folds from examples in the Rocky Mountain Basin and Range province, U.S.A, *J. Struct. Geol.*, *20*(7), 841–856, doi:10.1016/S0191-8141(98)00016-9.

John, B. E. (1987), Geometry and evolution of a mid-crustal extensional fault system: Chemehuevi Mountains, southeastern California, in *Continental Extensional Tectonics*, edited by M. P. Coward, J. F. Dewey, and P. L. Hancock, *Geol. Soc. London, Spec. Publ.*, *28*, 313–335.

Lasky, S. G., and B. N. Webber (1949), Manganese resources of the Artillery Mountains region, Mohave County, Arizona, *U.S. Geological Survey Bull.*, 961, 86 p.

Lucchitta, I., and N. H. Suneson (1993a), Dips and extension, *Geol. Soc. Am. Bull.*, *105*(10), 1346–1356, doi:10.1130/0016-7606(1993)105<1346:DAE>2.3.CO;2.

Lucchitta, I., and N. H. Suneson (1993b), Stratigraphic section of the Castaneda Hills-Signal area, Arizona, in *Tertiary Stratigraphy Of Highly Extended Areas, California, Arizona, and Nevada*, edited by D. R. Sherrod and J. E. Nielson, *U.S. Geol. Surv. Bull.*, *2053*, 139–144, Reston, Va.

Lucchitta, I., and N. H. Suneson (1994), Geologic map of the Centennial Wash Quadrangle, Mohave and La Paz Counties, Arizona, *U.S. Geological Survey Geologic Quadrangle Map*, GQ-1718, scale 1:24,000.

Marshak, S., and M. Vander Meulen (1989), Geology of the Battleship Peak area, southern Buckskin Mountains, Arizona: Structural style below the Buckskin detachment fault, in *Geology and Mineral Resources of the Buckskin and Rawhide Mountains, West-central Arizona*, *Arizona Geol. Surv. Bull.*, vol. 198, edited by J. E. Spencer and S. J. Reynolds, pp. 51–66, Arizona Geological Survey, Tucson.

Mirabella, F., F. Brozzetti, A. Lupattelli, and M. R. Barchi (2011), Tectonic evolution of a low-angle extensional fault system from restored cross-sections in the Northern Apennines (Italy), *Tectonics*, *30*, TC6002, doi:10.1029/2011TC002890.

Murphy, M. A., A. Yin, P. Kapp, T. M. Harrison, C. E. Manning, F. J. Ryerson, D. Lin, and G. Jinghui (2002), Structural evolution of the Gurla Mandhata detachment system, southwest Tibet: Implications for the eastward extent of the Karakoram fault system, *Geol. Soc. Am. Bull.*, *114*(4), 428–447, doi:10.1130/0016-7606(2002).

Nirrengarten, M., G. Manatschal, X. P. Yuan, N. J. Kusznir, and B. Maillot (2016), Application of the critical Coulomb wedge theory to hyper-extended, magma-poor rifted margins, *Earth Planet. Sci. Lett.*, *442*, 121–132, doi:10.1016/j.epsl.2016.03.004.

Prior, M. G., and J. S. Singleton (2016), Development of the Buckskin-Rawhide detachment fault system, west-central Arizona: Evidence from the sedimentary record, *Geol. Soc. Am. Abstracts Programs*, *48*(7), doi:10.1130/abs/2016AM-287831.

Prior, M. G., D. F. Stockli, and J. S. Singleton (2016), Miocene slip history of the Eagle Eye detachment fault, Harquahala Mountains metamorphic core complex, west-central Arizona, *Tectonics*, *35*, 1913–1934, doi:10.1002/2016TC004241.

Rehrig, W. A., and S. J. Reynolds (1980), Geologic and geochronologic reconnaissance of a northwest-trending zone of metamorphic core complexes in southern and western Arizona, in *Cordilleran Metamorphic Core Complexes*, *Geol. Soc. Am. Mem.*, vol. 153, edited by M. S. Crittenden Jr., P. J. Coney, and G. H. Davis, pp. 131–157, Boulder, Colo., doi:10.1130/MEM153-p131.

Reynolds, S. J., and J. E. Spencer (1985), Evidence for large-scale transport on the Bullard detachment fault, west-central Arizona, *Geology*, *13*(5), 353–356, doi:10.1130/0091-7613(1985)13<353:EFLTOT>2.0.CO;2.

Reynolds, S. J., and J. E. Spencer (1989), Pre-Tertiary rocks and structures in the upper plate of the Buckskin detachment fault, west-central Arizona, in *Geology and Mineral Resources of the Buckskin and Rawhide Mountains, West-central Arizona*, *Arizona Geol. Survey Bull.*, vol. 198, edited by J. E. Spencer and S. J. Reynolds, pp. 67–102, Tucson, Ariz.

Reynolds, S. J., F. P. Florence, J. W. Welty, M. S. Roddy, D. A. Currier, A. V. Anderson, and S. B. Keith (1986), Compilation of radiometric age determinations in Arizona, in *Arizona Bureau Geol. and Mineral Tech. Bull*, vol. 197, pp. 1–258, Tucson, Ariz.

Richard, S. M., J. E. Fryxell, and J. F. Sutter (1990), Tertiary structure and thermal history of the Harquahala and Buckskin Mountains, west-central Arizona: Implications for denudation by a major detachment fault system, *J. Geophys. Res.*, *95*(B12), 19,973–19,987, doi:10.1029/JB095iB12p19973.

Richard, S. M., T. C. Shipman, L. C. Greene, and R. C. Harris (2007), Estimated depth to bedrock in Arizona, *Arizona Geological Survey Digital Geologic Map*, DGM-52, scale 1:1,000,000, Tucson, Ariz.

Schlische, R. W. (1995), Geometry and origin of fault-related folds in extensional settings, *Am. Assoc. Petrol. Geol. Bull.*, *79*, 1661–1678.

Scott, R. J. (1995), The geological development of the Buckskin-Rawhide metamorphic core complex, west-central Arizona, PhD dissertation, Dept. Earth Sciences, Monash University, Melbourne, Victoria, Australia.

Scott, R. J. (2004), Geologic maps and cross sections of selected areas in the Rawhide and Buckskin Mountains, La Paz and Mohave Counties, Arizona, *Arizona Geological Survey Contributed Map*, CM-04-D, 10 sheets, Tucson, Ariz.

Scott, R. J., and G. S. Lister (1992), Detachment faults: Evidence for a low-angle origin, *Geology*, *20*(9), 833–836, doi:10.1130/0091-7613(1992)020<0833:DFEFAL>2.3.CO;2.

Scott, R. J., D. A. Foster, and G. S. Lister (1998), Tectonic implications of rapid cooling of lower plate rocks from the Buckskin-Rawhide metamorphic core complex, west-central Arizona, *Geol. Soc. Am. Bull.*, *110*(5), 588–614, doi:10.1130/0016-7606(1998)110<0588:TIORCO>2.3.CO;2.

Shackelford, T. J. (1989), Geologic map of the Rawhide Mountains, Mohave County, Arizona, in *Geology and Mineral Resources of the Buckskin and Rawhide Mountains, West-central Arizona*, *Arizona Geol. Surv. Bull.*, vol. 198, edited by J. E. Spencer and S. J. Reynolds, Arizona Geological Survey, Tucson.

Shafiqullah, M., P. E. Damon, D. J. Lynch, S. J. Reynolds, W. A. Rehrig, and R. H. Raymond (1980), K-Ar geochronology and geologic history of southwestern Arizona and adjacent areas, in *Studies in Western Arizona*, *Arizona Geol. Soc. Digest*, vol. 12, edited by J. P. Jenny and C. Stone, pp. 201–260, Arizona Geological Survey, Tucson.

Singleton, J. S. (2011), Geologic map and cross sections of the Little Buckskin Mountains, La Paz County, west-central Arizona, *Arizona Geol. Survey Contributed Map*, CM-11-B, scale 1:12,000, Tucson, Ariz.

Singleton, J. S. (2013), Geologic map and cross sections of the Swansea-Clara Peak Area, Buckskin Mountains, west-central Arizona, *Geol. Soc. Am. Map and Chart Series*, MCH104, scale 1:12,000.

Singleton, J. S. (2015), The transition from large-magnitude extension to distributed dextral faulting in the Buckskin-Rawhide metamorphic core complex, west-central Arizona, *Tectonics*, *34*, 1685–1708, doi:10.1002/2014TC003786.

Singleton, J. S., and S. Mosher (2012), Mylonitization in the lower plate of the Buckskin-Rawhide detachment fault, west-central Arizona: Implications for the geometric evolution of metamorphic core complexes, *J. Struct. Geol.*, *39*, 180–198, doi:10.1016/j.jsg.2012.02.013.

Singleton, J. S., E. Bird, and M. Hatfield (2014a), Geologic map of the Lincoln Ranch basin, Buckskin Mountains, west-central Arizona, scale 1:10,000, *Arizona Geological Survey Contributed Map*, CM-14-B, Tucson, Ariz.

Singleton, J. S., D. F. Stockli, P. B. Gans, and M. G. Prior (2014b), Timing, rate, and magnitude of slip on the Buckskin-Rawhide detachment fault, west central Arizona, *Tectonics*, *33*, 1596–1615, doi:10.1002/2013TC003517.

Spencer, J. E. (1989), Compilation geologic map of the Buckskin and Rawhide Mountains, west-central Arizona, in *Geology and Mineral Resources of the Buckskin and Rawhide Mountains, West-central Arizona*, *Arizona Geol. Surv. Bull*., vol. 198, edited by J. E. Spencer and S. J. Reynolds, Arizona Geological Survey, Tucson.

Spencer, J. E. (2010), Structural analysis of three extensional detachment faults with data from the 2000 Space-Shuttle Radar Topography Mission, *GSA Today*, *26*(8), 4–10, doi:10.1130/GSATG59A.1.

Spencer, J. E. (2011), Gently dipping normal faults identified with Space Shuttle radar topography data in central Sulawesi, Indonesia, and some implications for fault mechanics, *Earth Planet. Sci. Lett.*, *308*(3–4), 267–276, doi:10.1016/j.epsl.2011.06.028.

Spencer, J. E., and S. J. Reynolds (1989a), Middle Tertiary tectonics of Arizona and the Southwest, in *Geologic Evolution of Arizona*, *Arizona Geol. Soc. Digest*, vol. 17, edited by J. P. Jenney and S. J. Reynolds, pp. 539–574, Arizona Geological Survey, Tucson.

Spencer, J. E., and S. J. Reynolds (1989b), Tertiary structure, stratigraphy, and tectonics of the Buckskin Mountains, in *Geology and Mineral Resources of the Buckskin and Rawhide Mountains, west-central Arizona*, *Arizona Geol. Surv. Bull*., vol. 198, edited by J. E. Spencer and S. J. Reynolds, pp. 103–167, Arizona Geological Survey, Tucson.

Spencer, J. E., and S. J. Reynolds (1990), Geology and mineral resources of the Bouse Hills, west-central Arizona, *Arizona Geol. Survey Open-File Rep.*, 90–9, scale 1:24,000, Tucson, Ariz.

Spencer, J. E., and S. J. Reynolds (1991), Tectonics of mid-Tertiary extension along a transect through west-central Arizona, *Tectonics*, *10*, 1204–1221, doi:10.1029/91TC01160.

Spencer, J. E., and Y. Ohara (2014), Curved grooves at the Godzilla Megamullion in the Philippine Sea and their tectonic significance, *Tectonics*, *33*, 1028–1038, doi:10.1002/2013TC003515.

Spencer, J. E., S. J. Reynolds, and N. E. Lehman (1989a), Geologic map of the Planet-Mineral Hill area, northwestern Buckskin Mountains, west-central Arizona, in *Geology and Mineral Resources of the Buckskin and Rawhide Mountains, West-central Arizona*, *Arizona Geol. Surv. Bull*., vol. 198, edited by J. E. Spencer and S. J. Reynolds, Arizona Geological Survey, Tucson.

Spencer, J. E., M. Shafiqullah, R. J. Miller, and L. G. Pickthorn (1989b), K-Ar geochronology of Miocene extensional tectonism, volcanism, and potassium metasomatism in the Buckskin and Rawhide Mountains, in *Geology and Mineral Resources of the Buckskin and Rawhide Mountains, West-central Arizona*, *Arizona Geol. Surv. Bull*., vol. 198, edited by J. E. Spencer and S. J. Reynolds, pp. 184–189, Arizona Geological Survey, Tucson.

Spencer, J. E., M. J. Grubensky, J. T. Duncan, J. D. Shenk, J. C. Yarnold, and J. P. Lombard (1989c), Geology and mineral deposits of the Central Artillery Mountains, in *Geology and Mineral Resources of the Buckskin and Rawhide Mountains, West-central Arizona*, *Arizona Geol. Surv. Bull*., vol. 198, edited by J. E. Spencer and S. J. Reynolds, pp. 168–183, Arizona Geological Survey, Tucson.

Spencer, J. E., S. M. Richard, S. J. Reynolds, R. J. Miller, M. Shafiqullah, M. J. Grubensky, and W. G. Gilbert (1995), Spatial and temporal relationships between mid-Tertiary magmatism and extension in southwestern Arizona, *J. Geophys. Res.*, *100*(B6), 10,321–10,351, doi:10.1029/94JB02817.

Spencer, J. E., S. M. Richard, B. J. Johnson, D. S. Love, P. A. Pearthree, and S. J. Reynolds (2013), Geologic map of the Artillery Peak and Rawhide Wash 7 ½′ Quadrangles, Mohave and La Paz Counties, Arizona, *Arizona Geol. Survey Digital Geologic Map*, DGM-100, scale 1:24,000, Tucson, Ariz.

Spencer, J. E., A. Youberg, D. Love, P. A. Pearthree, T. R. Steinke, and S. J. Reynolds (2014), Geologic map of the Bouse and Ibex Peak 7 ½′ Quadrangles, La Paz County, Arizona *Arizona Geol. Survey Digital Geologic Map*, DGM-107, scale 1:24,000, Tucson, Ariz.

Strickland, E. D., J. S. Singleton, N. M. Seymour, and M. S. Wong (2016), Evidence for Orocopia Schist in the footwall of the Plomosa Mountains metamorphic core complex, west-central Arizona, *Geol. Soc. Am. Abstr. Programs*, *48*(7), doi:10.1130/abs/2016AM-283161.

Wernicke, B., and G. J. Axen (1988), On the role of isostasy in the evolution of normal fault systems, *Geology*, *16*(9), 848–851, doi:10.1130/0091-7613(1988)016<0848:OTROII>2.3.CO;2.

Wilkins, J., Jr., and T. L. Heidrick (1982), Base and precious metal mineralization related to low-angle tectonic features in the Whipple Mountains, California and Buckskin Mountains, Arizona, in *Mesozoic-Cenozoic Tectonic Evolution of the Colorado River Region, California, Arizona, and Nevada*, edited by E. G. Frost and D. L. Martin, pp. 182–203, Cordilleran Publishers, San Diego, Calif.

Wolfe, M. R., and D. F. Stockli (2010), Zircon (U–Th)/He thermochronometry in the KTB drill hole, Germany, and its implications for bulk He diffusion kinetics in zircon, *Earth Planet. Sci. Lett.*, *295*, 69–82, doi:10.1016/j.epsl.2010.03.025.

Xiao, H., and J. Suppe (1992), Origin of rollover, *Am. Assoc. Petrol. Geol. Bull.*, *76*(4), 509–529.

Xiao, H.-B., F. A. Dahlen, and J. Suppe (1991), Mechanics of extensional wedges, *J. Geophys. Res.*, *96*(B6), 10,301–10,318, doi:10.1029/91JB00222.

Yarnold, J. C. (1994), Tertiary sedimentary rocks associated with the Harcuvar core complex in Arizona (U.S.A.): Insights into paleogeographic evolution during displacement along a major detachment fault, *Sediment. Geol.*, *89*(1–2), 43–63, doi:10.1016/0037-0738(94)90083-3.